



SIATS Journals

**Journal of Experimental & Theoretical
Nanotechnology Specialized Researches**

(JETNSR)

Journal home page: <http://www.siats.co.uk>



The effect of additives on behavior of the high temperature

$\text{La}_x\text{Y}_{1-x}\text{Ba}_2\text{Cu}_3\text{O}_{7-\delta}$ superconductor

Alhuthari Abdulbaqi Ali¹, Widad Mahmood Faisal¹, Salwan K. J. Al-Ani^{2,*}

**¹Department of Electronic & Communication, Faculty of Engineering &
Petroleum, Hadramout University, Hadramout, Yemen**

**²Department of Physics, College of Science, University of Baghdad, Baghdad,
Iraq**

salwan_kamal@yahoo.com

ARTICLE INFO

Article history:

Received 28/5/2015

Received in revised form 9/7/2015

Accepted 16/2/2016

Available online 15/1/2017

Keywords: *High temperature superconductor; $\text{La}_x\text{Y}_{1-x}\text{Ba}_2\text{Cu}_3\text{O}_{7-\delta}$; X-ray diffraction; Resistivity measurement; Critical temperature.*

PACS: *74.25.-q; 61.05.cp; 84.37.+q; 74.10.+v; 74.62.-c.*

Abstract

A series of ceramic superconductor compounds with the composition $\text{La}_x\text{Y}_{1-x}\text{Ba}_2\text{Cu}_3\text{O}_{7-\delta}$ are prepared by solid state reaction from the principle routs like La_2O_3 , BaCO_3 and CuO with high purity 99.99%. Different measurement are made to show the improvement in high phase superconductor such as resistivity measurement and the X-ray diffraction (XRD). When ($x=0.20$



and 0.80; $x=0.40$ and 0.60) an orthorhombic phase is appeared with lattice constants ($a= 3.844 \text{ \AA}$, $b=3.912 \text{ \AA}$, $c=11.839 \text{ \AA}$) and ($a= 3.871 \text{ \AA}$, $b=3.881 \text{ \AA}$, $c=11.748\text{\AA}$), respectively. This emphasizes the formation of a high temperature superconducting phase. At $x=0.5$ a phase is changed to a tetragonal where the superconductivity is lost. From the resistivity measurement, the highest (T_c) value is found equals to (97K) for ($x=0.20$ and $x=0.80$) comparable with the YBCO-compound which does not normally exhibited T_c -value greater than (95K). The increase in T_c -value may be attributed to the amount of (La) and / or the oxygen content in the mixture which both influence the properties of the compound and are essential for the superconductivity phase.

1. Introduction

The detection of the so-called High Temperature Superconductor (HTS) in 1986 by Bednorz and Muller [1] dramatically changed the prospect of electrical power applications of superconductors, because of the significantly increased critical temperature, T_C , in which the employment of a more economical cryogen, liquid nitrogen becomes possible. Between 1987 and 1993, T_C is raised from 92 K as revealed in $YBa_2Cu_3O_x$ (YBCO) [2]. Moreover 130 K is as demonstrated in $Hg_2Ba_2Ca_2Cu_3O_y$ [3]. Meanwhile, extensive efforts have been directed to develop practical HTS conductors with high current carrying capability. First, concentrating on Bi-2223 ($Bi_2Sr_2Ca_2Cu_3O_z$) and recently on YBCO-123 based coated conductor, referred to as “2nd generation conductor”. With low losses and high current carrying capability, HTS conductors allows electrical devices to be built with higher efficiency and higher power density. It also enables novel devices such as Superconducting Magnetic Energy Storage (SMES), magnetic bearings, fault current limiters and switches [4]. Furthermore, HTS offers environmental advantages; oil free transformers and devices with low magnetic field leakage. In the hope of a large scale HTS application in electrical power industry, significant public and private programmers have been initiated both to accelerate conductor development and to build prototypes in the USA, Europe, and Japan.

HTS represents a new class of conductor with unique properties, which not only allows electric power devices to be more compact but also enables new applications. The conductors developed so far have enabled various power device prototypes, such as power cables [6-8], transformers [9,10], motors [11,12], and Superconducting Fault Current Limiters (SCFCL) [13-15].



As compared with common superconducting materials such as $\text{YBa}_2\text{Cu}_3\text{O}_y$, La-based high-temperature superconducting (HTSC) possess some attracting features, such as high superconducting critical temperature (T_C), high critical current density (J_C), very low microwave surface resistance (R_s) and a good stability in moisture [16–20]. All of these properties merit potential superiority of La-based thin-film devices for electronic applications, ranging from superconducting quantum interference devices (SQUIDs) to superconducting microwave resonators and also other passive devices [21–26]. The effects of partial substitution of Y by La – atom on the growth mechanism and superconducting properties will be studied for the component $\text{La}_x\text{Y}_{1-x}\text{Ba}_2\text{Cu}_3\text{O}_{7-\delta}$ at $x=0, 0.20, 0.40, 0.50, 0.60$ and 0.80 .

2. Experimental Procedure

The samples are prepared by using the standard solid-state reaction technique. The detailed procedures for the sample preparation are as follows; pure cation oxides of Y_2O_3 (99.995%), La_2O_3 (99.99%), BaCO_3 (99.99%), and CuO (99%) are weighted and mixed according to the chemical formula of $\text{YBa}_2\text{Cu}_3\text{O}_{7-y}$ (YBCO) and $\text{La}_x\text{Y}_{1-x}\text{Ba}_2\text{Cu}_3\text{O}_{7-\delta}$ with $x=0, 0.20, 0.40, 0.50, 0.60$ and 0.80 .

In order to make, the specimens mixture is prepared by homogeneously mixing and grinding prescribed amounts of powders into a gate mortar. Appropriate amounts of these powders are mixed with alumina mortar and pestle for (2 hours) in 2- propanole and dried. They are put into a furnace (Nabartherm-N11/R) and calcined at 930°C in air for 48 hrs. This process is repeated three times. Then, the final step of the sample preparation is undergone to high temperature treatment that leads the particles to join together and gradually reduce the volume of pore space between them. The powder is compacted into a pellet shape with a certain pressure. After that, the powder particles will then be in contact with one another at numerous sites, with significant amount of pore space between the particles. In order to reduce the boundary energy, atoms diffuse to the boundaries, permitting the particles to be bound together and eventually causing shrinkage in the pores. However, if sintering is carried out for a long time the pores may be eliminated and the material becomes dense.

The calcined powders are pulverized and reground pelletized into disk-shaped pellets. The die has a stainless steel cylinder of 0.5 cm (13 mm) diameter and 1.5-1.8 mm thick using manually hydraulic press RAKIN-EIMER, under a pressure of 8 ton/cm^2 (0.6 Gp). The programming data for this process includes; the rate of heating ($60^\circ\text{C}/\text{hour}$) up to (930°C) for 30 hours with the flow



of oxygen gas of about 1.25 L/min and then with slow rate of cooling (30 °C/hours). The temperature is, afterwards, decreased down to about 550°C with 4 °C /min and kept at this level for 12 hrs in oxygen flow to enhance the value of δ to reach the content of oxygen atoms in the samples to about (6.85) before returning to a room temperature. Finally, the products are cooled down to a room temperature.

2.1. X-Ray diffraction

The structural characterization is performed by X-ray diffraction (XRD). While the X-ray powder diffractometry is generally dealing exclusively with crystalline (order) materials. X-ray patterns are used for initial identification of lattice type as the unit of crystal structure and the building block for the materials with acknowledge of the chemical composition ionic size, lattice parameters, structure model can be built X-Ray diffraction pattern can be utilized to determine the phase present in the sample by observing the intensity peaks in relation to its (hkl) values. Based on the determination of Miller indices, hkl, and the lattice parameters for all the orthogonal crystal systems are calculated as the following. For cubic system, $a=b=c$

$$\frac{1}{d_{hkl}^2} = \frac{h^2 + k^2 + l^2}{a^2} \quad (1)$$

For tetragonal system, $a=b \neq c$

$$\frac{1}{d_{hkl}^2} = \frac{h^2 + k^2}{a^2} + \frac{l^2}{c^2} \quad (2)$$

and for orthorhombic system, $a \neq b \neq c$

$$\frac{1}{d_{hkl}^2} = \frac{h^2}{a^2} + \frac{k^2}{b^2} + \frac{l^2}{c^2} \quad (3)$$

In this work, (XRD) type PHILIPS with the following features; the source Cu K α I, current 20 mA, Voltage 40 kV and $\lambda=1.5405 \text{ \AA}$ are used. The X-ray chart and ASTM-data [27] are used in a computer program to analysis the X-ray data in order to refine the structure of the sample conducted in this study and to obtain the lattice constants.



2.2. Sample Testing

The critical temperature of the superconducting sample is measured by using the four-point probe technique which is considered as a suitable method for studying the electrical behavior of superconducting materials. In this method, a small current passed through a sample and the voltage drop across it. The terminals distinct from those utilized for passing the main part of the current through the specimen, where voltage drop in both leads and contacts are the electrical contact to the sample which are made with fine copper wires adhered with silver paste. The cryostat system is used for the measurement of critical resistivity of the sample with the present of a liquid Nitrogen. The cryostat is joined to a rotary pump to get a pressure of $\sim 10^{-2}$ mbar inside the cryostat.

3. Result and Discussions

3.1. Structure properties of $La_xY_{1-x}Ba_2Cu_3O_{7-\delta}$

All samples of partial substitution of Y by La –atom are examined by powder XRD and the typical XRD -2θ patterns are presented in Fig's 1, 2, 3, and 4, respectively. These results indicate that there are a good crystalline which textured with the *c*-axis perpendicular to the surface of the substrate. The four sharp peaks are consistent in intensity and shifted by 90° from one peak to another indicating the fourfold symmetry of the La-2212 crystal. To examine the presence of superconductivity phase, the structure nature of orthorhombic phase for all samples under study with ($x=0, 0.20, 0.40, 0.60$ and 0.80) is investigated.

The X-ray analyses show that all the compounds exhibit essentially *c*-axis oriented with good crystalline may not relate closely to the initial substrate conditions. Due to La substitution in Y with some modifications in the peaks appear represented by their intensity or positions. The effect of substitution of La on the Y with the concentration ($x=0.20, x=0.80$) is presented in Fig. 1. When substituting Y by La for the component $La_xY_{1-x}Ba_2Cu_3O_{7-\delta}$ for $x=0, 0.20, 0.40, 0.50, 0.60, 0.80$ show a gradual transfer the orthorhombic phase to a tetragonal at $x=0.50$.

When $x=0.20$ and $x=0.8$, the HTS exhibits an orthorhombic phase with a lattice cell constants $a=3.844 \text{ \AA}$, $b=3.912 \text{ \AA}$, $C=11.839 \text{ \AA}$ as shown in Fig. 1. The lattice parameters, unit cell volume and orthorhombicity are listed in Table I. The increase in the *c* parameter is significant and is indicative of the Y replacement by La. This, however, does not guarantee the absence of partial



Ba substitution by La. A smaller unit cell volume for $x=0.1$ is similar to the results of Liang et al. [28] who observed a decreasing trend in the unit cell volume for increasing Ba substitution by La.

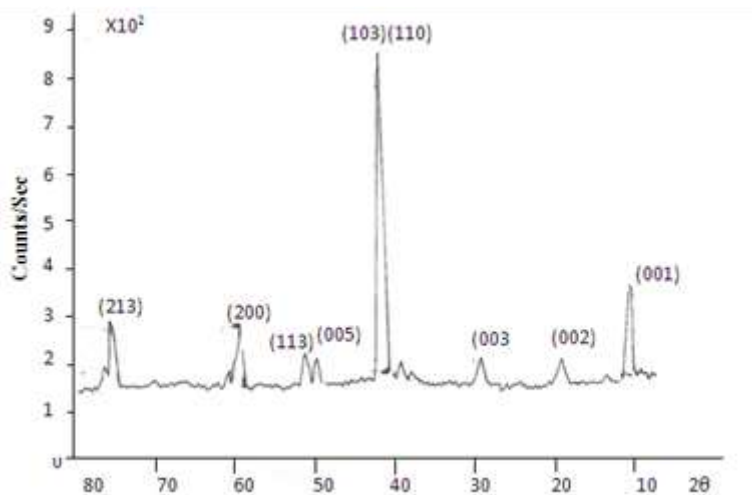


Fig. 1: X-ray diffraction for the component $\text{La}_x\text{Y}_{1-x}\text{Ba}_2\text{Cu}_3\text{O}_{7-\delta}$ for $x=0.2$, $x=0.8$ with oxygen vacuum in temperature $930\text{ }^\circ\text{C}$.

When $x=0.4$ and $x=0.6$, it exhibits an orthorhombic phase with a lattice cell parameters; $a=3.871\text{ \AA}$, $b=3.881\text{ \AA}$, $c=11.748\text{ \AA}$ as shown in Fig. 2.

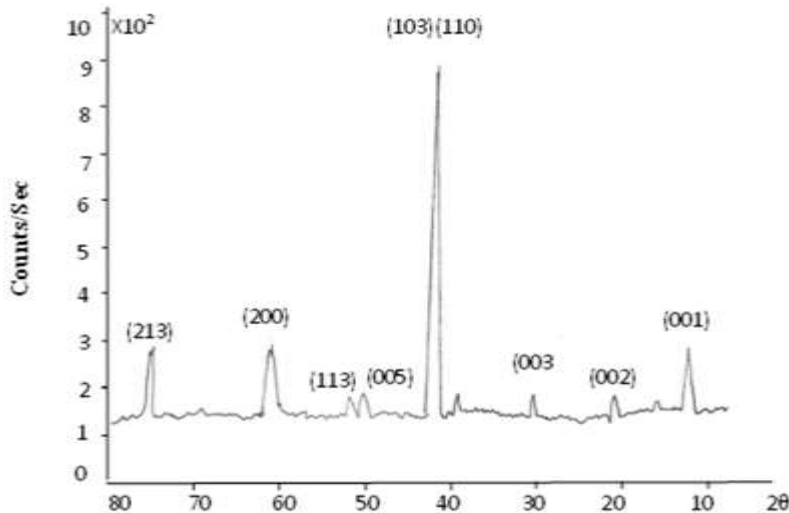


Fig. 2: X-ray Diffraction for the component $\text{La}_x\text{Y}_{1-x}\text{Ba}_2\text{Cu}_3\text{O}_{7-\delta}$ for $x=0.4$, $x=0.6$ with oxygen vacuum in temperature $930\text{ }^\circ\text{C}$.



At last $x=0.50$ is orthorhombic phase lattice cell $a=b= 3.876 \text{ \AA}$, $c=11.743 \text{ \AA}$ as shown in Fig. 3.

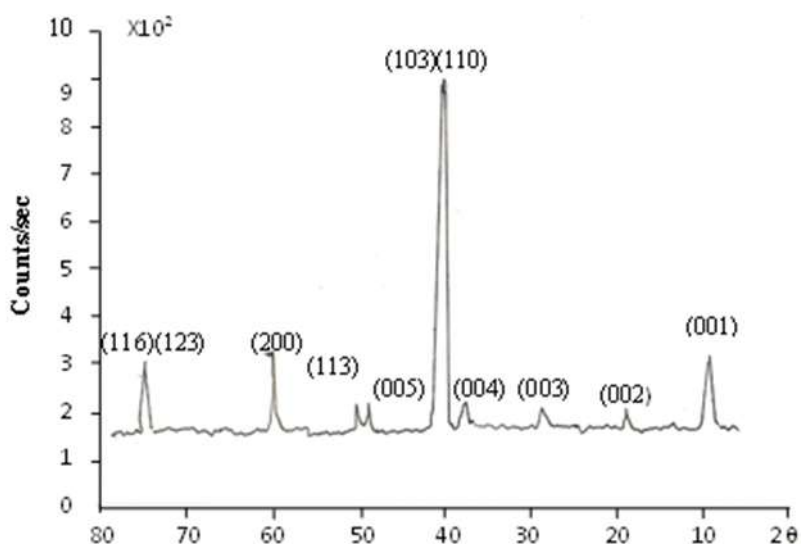


Fig. 3: X-ray Diffraction for the component $\text{La}_x\text{Y}_{1-x}\text{Ba}_2\text{Cu}_3\text{O}_{7-\delta}$ for $x=0.5$ with oxygen vacuum in temperature $930 \text{ }^\circ\text{C}$.

While the $x=0.5$ sample shows loss of superconductivity, this behavior, similar to that of $\text{Y}(\text{La}_x\text{Ba}_{1-x})\text{Cu}_3\text{O}_7$ samples reported earlier [28,29], which consists of a decrease in T_c as x ($\text{La}_x\text{Y}_{1-x}\text{Ba}_2\text{Cu}_3\text{O}_{7-\delta}$) is increased and a disappearance of superconductivity at $x \approx 0.5$. This similarity in the variation of superconducting properties with the lanthanum content suggests the possibility of lanthanum substitution for barium and the concomitant mixing of the La and Ba sites in our samples. From the neutron diffraction studies such a mixing is known to occur in $\text{LaBa}_2\text{Cu}_3\text{O}_7$ [30]. Thus, the behavior of the solid solutions seems to be guided by the substitution of La into the Ba sites along with the Y sites. When $x=0$, it gives the structure $\text{YBa}_2\text{Cu}_3\text{O}_{7-\delta}$ with lattice constants; $a= 3.842 \text{ \AA}$, $b=3.912 \text{ \AA}$, $c=11.752 \text{ \AA}$ as shown in Fig. 4.



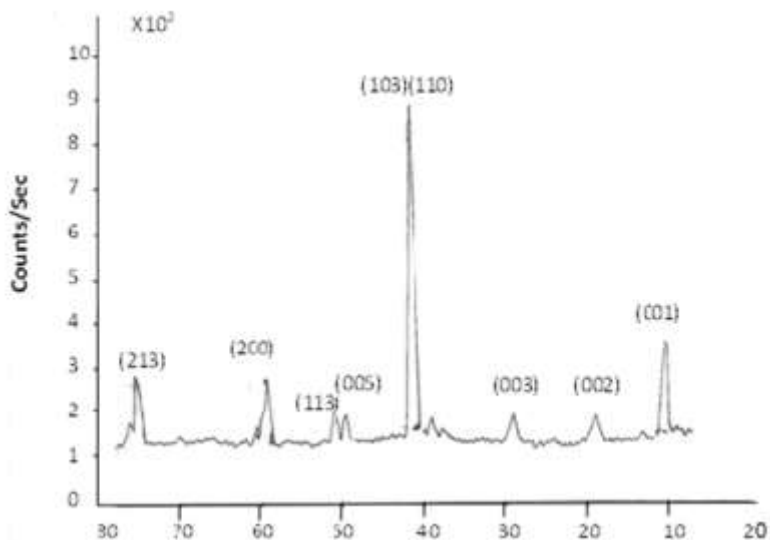


Fig. 4: X-ray Diffraction for the component $\text{La}_x\text{Y}_{1-x}\text{Ba}_2\text{Cu}_3\text{O}_{7-\delta}$ for $x=0$ with oxygen vacuum in temperature 930°C .

The X-ray diffraction pattern of this sample shows the splitting of the (200) and (005) reflections, though the resistivity behavior is still semiconducting. Thus, the importance of proper oxygen stoichiometry in addition to the orthorhombic structure for the occurrence of superconductivity in the 123 system is evident.

3.2. Resistivity properties of $\text{La}_x\text{Y}_{1-x}\text{Ba}_2\text{Cu}_3\text{O}_{7-\delta}$

The zero field resistivity as a function of temperature for the nominal compositions $\text{La}_x\text{Y}_{1-x}\text{Ba}_2\text{Cu}_3\text{O}_{7-\delta}$ ($x = 0, 0.20$ and 0.40) are shown in Fig's 5, 6 and 7 (the lower inset shows the resistivity over a larger range of temperature) measured by standard four probe method. The resistivity decreases monotonously with decreasing temperature and the onset of superconducting transition occurs at 95, 97 and 96 K for $x = 0, x = 0.20$ and $x = 0.40$ compositions respectively.

For $x = 0.20$ and $x = 0.40$, the transition is rather broad and the T_c values are approximate. This enhancement in T_c indicates that small amount of Yttrium is substituted at the La sites. The smaller size of Yttrium (atomic radius 180 pm) as compared to lanthanum (atomic radius 195 pm) leads to subtle changes in the bandwidth and this probably enhances the superconducting transition temperature. Nevertheless, in compositions with higher Yttrium ratio, the superconducting transition temperature decreases and the transition broadens which suggests the compositional dependence of T_c . whereas, at $x=0.5$ the composition is losing its superconductivity. It is known that a small changes in the crystalline structure of a high temperature cuprate superconductor



(HTCS) produce large changes in its magnetic properties [31]. The structural changes are produced by chemical substitutions of cations or anions. Thus, altering the position and occupancy of the atoms situated in the superconducting planes CuO_2 and also leads to increasing (or decreasing) the superconducting critical temperature (T_c). Indeed Luis et al [31] reported that by changing the oxygen content in the superconductor $\text{YBa}_2\text{Cu}_3\text{O}_7$ (YBCO-7) to ≤ 6.4 , the occupancy of the oxygen situated in the Cu-O chains decreases and the crystalline structure changes from orthorhombic to tetragonal where the superconductivity is destroyed.

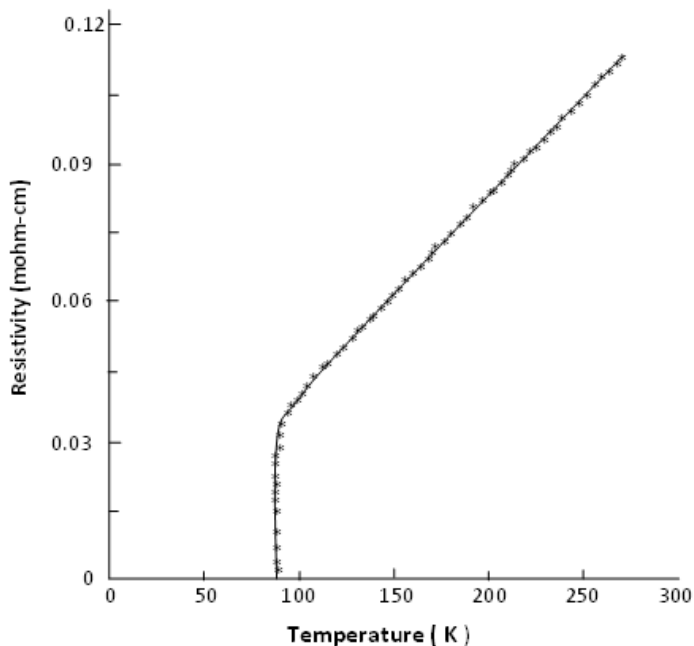


Fig. 5: The resistivity versus temperature for HTSC $\text{La}_x\text{Y}_{1-x}\text{Ba}_2\text{Cu}_3\text{O}_{7-\delta}$.

The relation of resistivity vs. temperature curve for the concentration $x=0$ is shown in Fig. 5 with $T_c=95\text{K}$. While, the critical temperature is increased when the concentration $x=0.2$ and $x=0.8$; $T_c = 97\text{K}$ and at $x=0.4$; $T_c = 96\text{K}$ as shown in Fig. 6.



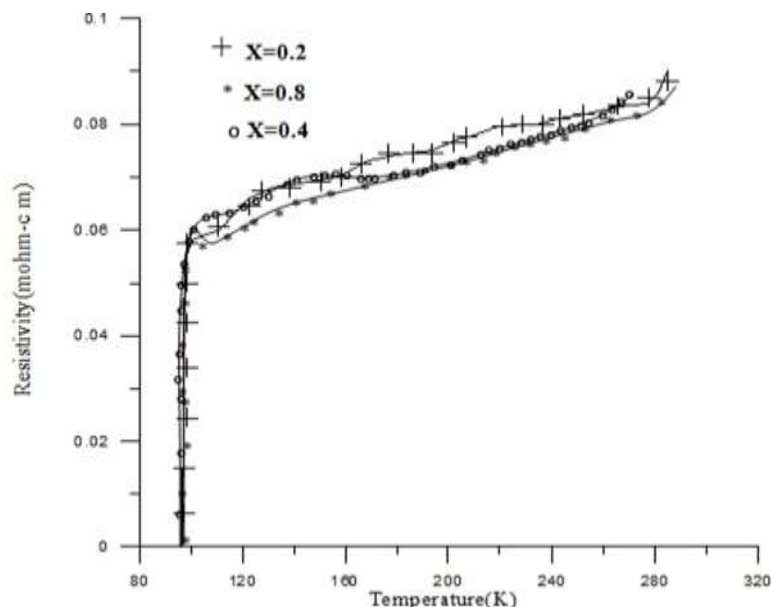


Fig. 6: The resistivity versus temperature for HTSC $\text{La}_x\text{Y}_{1-x}\text{Ba}_2\text{Cu}_3\text{O}_{7-\delta}$ for $x=0.2$, $x=0.8$

The resistivity dropped suddenly with concentration $x=0.6$ [$T_c=83\text{K}$], which is due to (La) substitution in the mixture and hence affects the T_c values as shown in Fig. 7. The values of T_c for different components of $\text{La}_x\text{Y}_{1-x}\text{Ba}_2\text{Cu}_3\text{O}_{7-\delta}$ superconductor are listed in Table I. Ganapathi et al. [30] earlier found for $x \leq 0.5$ the $\text{La}_x\text{Y}_{1-x}\text{Ba}_2\text{Cu}_3\text{O}_{7-\delta}$ system behaves like a pure Y_{123} superconducting oxide with T_c onset equal to 90 K. They obtained a maximum $T_c = 94$ K (zero resistance at 91 K) when $x=0.1$. For $x > 0.5$ they reported that the system starts to behave like a La_{123} . The changes in the values of the T_c in the present system are due to changes in oxygen sites in chains and levels of CuO. These changes depend on the partial compensation of (CuO_2) . The difference in these sites has caused confusion in the paths of Cooper pairs.



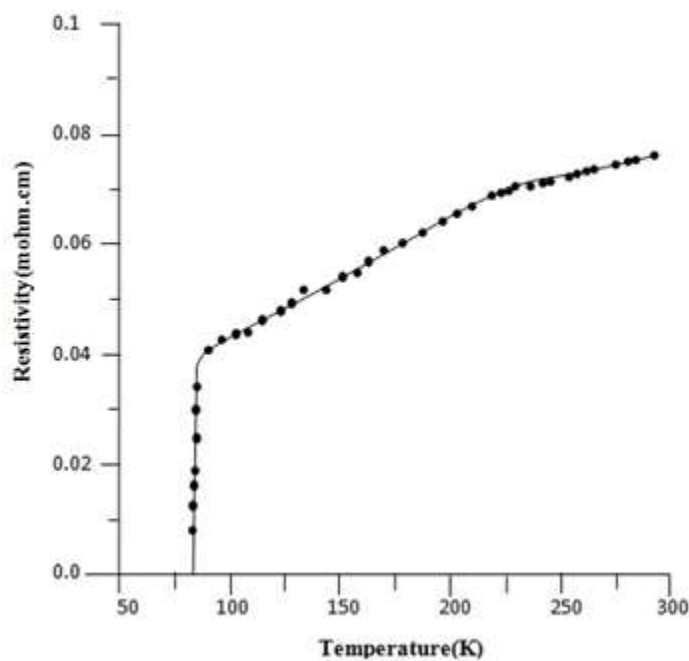


Fig. 7: The resistivity versus temperature for HTSC $\text{La}_x\text{Y}_{1-x}\text{Ba}_2\text{Cu}_3\text{O}_{7-\delta}$ for $x = 0.6$

Table 1: The values of the lattice constants and the T_c for different components of $\text{La}_x\text{Y}_{1-x}\text{Ba}_2\text{Cu}_3\text{O}_{7-\delta}$ superconductor.

Samples	T_c (K) Onset	Lattice Constants
$\text{La}_x\text{Y}_{1-x}\text{Ba}_2\text{Cu}_3\text{O}_{7-\delta}$ for $x=0$	95 K	$a= 3.842$ $b=3.912$ $c=11.752$
$\text{La}_x\text{Y}_{1-x}\text{Ba}_2\text{Cu}_3\text{O}_{7-\delta}$ for $x=0.20$	97 K	$a= 3.844$ $b=3.912$ $c=11.839$
$\text{La}_x\text{Y}_{1-x}\text{Ba}_2\text{Cu}_3\text{O}_{7-\delta}$ for $x=0.40$	96 K	$a= 3.871$ $b=3.881$ $c=11.748$
$\text{La}_x\text{Y}_{1-x}\text{Ba}_2\text{Cu}_3\text{O}_{7-\delta}$ for $x=0.50$	the component loses superconductivity	$a=3.876$ $b= 3.876$ $c=11.743$
$\text{La}_x\text{Y}_{1-x}\text{Ba}_2\text{Cu}_3\text{O}_{7-\delta}$ for $x=0.60$	83K	$a= 3.871$ $b=3.881$ $c=11.748$
$\text{La}_x\text{Y}_{1-x}\text{Ba}_2\text{Cu}_3\text{O}_{7-\delta}$ for $x=0.80$	97K	$a= 3.844$ $b=3.912$ $c=11.839$



4. Conclusions

This study shows that the growth mechanism and hence the resulting structural and superconducting properties are significantly affected by the substitution of Y - atoms by La atoms in $\text{La}_x\text{Y}_{1-x}\text{Ba}_2\text{Cu}_3\text{O}_{7-\delta}$ compound for $x=0, 0.2, 0.4, 0.5, 0.6, 0.8$ and gradually transfer of the orthorhombic phase to the tetragonal phase when $x=0.5$. The present results have important implications that substitution can be used to control the microstructure and surface morphologies of YBCO compound. The superconductivity of the solid solution $\text{La}_x\text{Y}_{1-x}\text{Ba}_2\text{Cu}_3\text{O}_{7-\delta}$ is a strong function of x . Lanthanum occupies both Y and Ba sites and the extent of Ba substitution by La controls the properties of the system. Samples with $0 \leq x \leq 0.8$ are orthorhombic with decreasing orthorhombicity as a function of x . The unit cell volume increases as $x = 0.2$ and $x=0.8$. Two distinct behaviors are observed in the electrical characteristics of the solid solutions. For $x = 0.2$ and $x=0.8$ the solid solution behaves similarly to the $x=0$ a member with a metallic behavior followed by a superconducting transition at $T_c = 95$ K. A slightly higher $T_c = 96$ K for the $x=0.4$ sample behavior followed by a superconducting transition at $x=0.6$, $T_c = 83$ K [26,32]. The orthorhombic structure and optimum oxygen content are found to be essential for the observation of superconductivity in the 123 system. Interestingly, these two parameters are independent variables in the La-rich compounds, unlike the pure Y_{123} compound.

References

- [1] G. Bednorz, K.A. Muller, *Zeitschrift für Physik B* **64** (1986) 189
- [2] M.K. Wu, J.R. Ashburn, C.J. Torng, P.H. Hor, R.L. Meng, L. Gao, Q. Huang, C.W. Chu, *Physical Review Letter* **58** (1987) 908
- [3] A. Schilling, M. Carboni, J. Guo, H.R. Ott, *Nature* **363** (1993) 56
- [4] B. Seeber, *Handbook of Applied Superconductivity*, OIP Publishing, Bristol (1998)
- [5] M. Chen, L. Donzel, M. Lakner, W. Paul, *Journal of the European Ceramic Society* **24** (2004) 1815
- [6] T. Masuda, Y. Ashibe, M. Watanabe, C. Suzawa, K. Ohkura, Hirose, Y. Takahashi, *Physica C* **372-376** (2002) 1580
- [7] J.P. Stovall, J.W. Lue, J.A. Demko, P.W. Fisher, M.J. Gouge, R.A. Hawsey, J.W. Armstrong, R.L. Huges, J.C. Tolbert, *Advances in Cryogenic Engineering* **47** (2002) 591
- [8] D. Willen, F. Hansen, M. Daumling, C.N. Rasmussen, C. Traeholt, S.D. Mikkelsen,



Physica C **372-376** (2002) 1571

- [9] R. Schlosser, M. Meinert, M. Leghissa, IEEE Transactions on Applied Superconductivity **2** (2003) 2348
- [10] P.G. Therond, C. Levillain, J.F. Picard, B. Bugnon, H. Zeuger, S. Hornfeldt, T. Fogelberg, G. Papst, D. Bonmann, Proceeding of 37th Cigre Session pp. 302 (1998)
- [11] M. Frank, J. Frauenhofer, P. van Hasselt, W. Nick, H.-W. Neumueller, G. Nerowski, Ieee Transactions on Applied Superconductivity **13** (2003) 2120
- [12] D. Madura, M. Richardson, D. Bushko, S. Kalsi, B. Gamble, The Applied Superconductivity Conference, IEEE (2002)
- [13] W. Paul et al. Superconductor Science & Technology **10** (1997) 914
- [14] W. Paul, M. Chen, M. Lakner, J. Rhyner, D. Braun, W. Lanz, Physica C **354** (2001) 27
- [15] R. Witzmann, W. Schmidt, R. Volkmar, ETG-Fachberichte Band **85** (2001) 393
- [16] D. S. Ginley, TI-based HTSC films for microelectronic applications Thallium-Based High-Temperature Superconductors. Ed. A. M. Hermann and S. V Yakhmi (New York: Marcel Dekker) chapter 9 (1993)
- [17] A.P. Bramley, J. D. O'Connor, C. R. M. Grovenor, Supercond. Sci. Technol. **12** (1999) R57
- [18] H. Schneidewind, M. Manzel, G. Bruchlos, K. Kirsch, Supercond. Sci. Technol. **14** (2001) 200
- [19] S. Huber, M. Manazel, H. Bruchlos, S. Hensen, G. Muller, Physica C **244** (1995) 337
- [20] W. L. Holstein, L. A. Parisi, C. Wilker, R. B. Flippen, Appl. Phys. Lett. **60** (1992) 2014
- [21] Y. F. Chen, Z. G. Ivanov, E. A. Stepanov, A. Ya. Tzalenchuk, S. Zarembinski, T. Claeson, L-G. Johansson, J. Appl. Phys. **79** (1996) 9221
- [22] W. L. Holstein, L. A. Parisi, Z-Y. Shen, C. Wilker, M. S. Brenner, J. S. Martens J. Supercond. **6** (1993) 191
- [23] A. Cassinese, A. Andreone, E. Di Gennaro, G. Pica, R. Vaglio, G. Malandrino, L. M. S. Perdicaro, I. L. Fragala, C. Granata, Supercond. Sci. Technol. **14** (2001) 406
- [24] M. Barra, A. Cassinese, I. Fragala, M. Kusunoki, G. Malandrino, T. Nakaggawa, L. Perdicaro, K. Sato, S. Oshima, R. Vaglio, Supercond. Sci. Technol. **15** (2002) 581
- [25] D. Face, M. Frank, J. Robert, B. Likie, S. Mark, W. Charles, IEEE Trans. Appl. Supercond. **9** (1999) 2492
- [26] D. S. Ginley, E. L. Venturini, C. P. Tigges, T. E. Zipperian, R. J. Baughman, J. C. Barbour, B. Morosin, Physica C **185** (1991) 2275



- [27] J. Xiaoping, Z. Xiaobiao, P. Dexing, Q. Hongbo, Y. Zhoujin, Y. Huafeng, Z. Xizhang, L. Shuzhi, Q. Guiwen; *J. Phys. C, Solid state Physics* **20** (1987) L533
- [28] R. Liang, M. Itoh, T. Nakamura and R. Aoki, *Physica C* **157** (1989) 83
- [29] T.C. Huang, Y. Tokura, J.B. Torrance, A.I. Nazzal and R. Karimi, *Appl. Phys. Lett.* **52** (1988) 1901
- [29] A. Sequeria, H. Rajagopal, L. Ganapathi and C.N.R. Rao, *J. Solid State Chem.* **76** (1988) 235
- [30] L. Ganapathi, Ashok Kumar and J. Narayan, *Fundamental Properties and Novel Materials*, Vol. 169, 561-564, *Proceeding of Materials Research Society* (1989)
- [31] V. Luis De Los Santos, D. Angel Bustamante, J. C. Gonzalez, L. Juan Feijoo, A. Ana Osorio, T. Mitrelias, Y. Majima, Crispin H.W. Barnes, *The Open Superconductivity Journal* **2** (2010) 19
- [32] A. Manthiram, X.X. Tang, J. B. Goodenough, *Phys. Rev. B* **37** (1988) 3734

